Rotational spectra and structure of the floppy C_2H_4–H_2S complex: bridging hydrogen bonding and van der Waals interactions

M. Goswami, P.K. Mandal, D.J. Ramdass, E. Arunan *

Department of Inorganic and Physical Chemistry, Indian Institute of Science, 138, IPC Department, Bangalore 560 012, India

Abstract

This Communication reports the rotational spectrum of a weakly bound C_2H_4–H_2S complex which appears to be a composite of rotational spectra of the hydrogen bonded C_2H_4–H_2O and the van der Waals complex C_2H_4–Ar, reported earlier. Each transition is split in to four with a smaller splitting of about 0.14 MHz and a larger splitting of 1.67 MHz in $(B + C)/2$. Results for D_2S and HDS isotopomers suggest that the smaller splitting is due to C_2H_4 tunneling and the larger splitting is due to internal rotation of H_2S. The equilibrium structure shows S–H$\cdots\pi$ bonding.
© 2004 Elsevier B.V. All rights reserved.

1. Introduction

Intermolecular interactions have attracted enormous interest in the recent decades. Studies on 'hydrogen bonded' and 'van der Waals' complexes in the gas phase have been leading to important fundamental information about intermolecular potentials [1,2]. The terms 'hydrogen bonding', electrostatic interactions and 'van der Waals interactions' are loosely and interchangeably used. For example, Dunning [3] does not consider the N_2–HF as hydrogen bonded complex (it is included as an example for electrostatic interaction different from hydrogen bonding) and Bader [4] identifies the Ar–HF as hydrogen bonded complex. According to the IUPAC definition [5], N_2–HF would be hydrogen bonded and Ar–HF is left to the imagination of individuals. The IUPAC definition for hydrogen bond suggests that the two atoms X and Y involved in hydrogen bonding as in X–H$\cdots$Y are 'usually (but not necessarily) from the first row of Periodic Table i.e. N, O or F'. IUPAC's definition also states that hydrogen bonding is best considered as an electrostatic interaction. This may be contrasted with the van der Waals (dispersion) forces leading to the name of van der Waals complexes.

There has been a debate about the similarities and differences between the hydrogen bonded complexes formed by first row (HF, H_2O) and second row (HCl, H_2S) hydrides [6,7]. Tao and Klemperer [6] argue that dispersion plays a more important role in $(HCl)_2$ than in $(HF)_2$. On the other hand, Augspurger and Dykstra [7] highlight the importance of electrostatic interactions in a series of HCl complexes. Experimental results on 'hydrogen bonded complexes' of second row hydrides can provide useful data for better understanding of weak interactions.

There have been numerous investigations on HF, H_2O and HCl complexes in the gas phase but relatively few H_2S complexes have been investigated. A systematic analysis of the structural parameters of HF, HCl and H_2O complexes led us to define a hydrogen bond radius for these and some other H bond donors [8,9]. Hence, our laboratory has been investigating the rotational spectra of various H_2S complexes, using a pulsed nozzle Fourier transform microwave spectrometer. The S–H group as hydrogen bond donor is important in the amino acid cysteine and its derivatives [10]. This communication discusses the rotational spectrum of C_2H_4–H_2S complex. Ab initio calculations at the MP2/6-311++G** level are reported as well and there is a reasonable agreement between experimental and theoretical structures.

* Corresponding author. Fax: +918023601552.
E-mail address: arunan@ipc.iisc.ernet.in (E. Arunan).

2. Experimental and computational details

The pulsed nozzle Fourier transform microwave spectrometer used in this study has been described in detail elsewhere [9]. The basic design is that of Balle and Flygare [11] and many of the recent advances [12–14] in design have been implemented. The title complex was formed in a supersonic expansion with Ar as the carrier gas. The back pressure was typically 0.5 atm and the microwave pulse was of 0.5 μs duration. The identity of the complex was established by ensuring the presence of C_2H_4 and H_2S and also by observing the signal with Helium as carrier gas, with a backing pressure of 1 atm. Strong signals were observed for the $C_2H_4–H_2S$ complex which could be readily seen in a single shot. The $C_2H_4–H_2^{34}S$ transitions could be seen in natural abundance. The HDS/D_2S isotopomers were observed by flowing H_2S through either a H_2O/D_2O mixture or pure D_2O, respectively. All gases have been obtained from Bhoruka Gases Ltd and used as supplied: Ar (99.999%), C_2H_4 (99.9%) and H_2S (99.5%). D_2O (99.5% D) was obtained from Aldrich.

Ab initio calculations have been carried out using GAUSSIAN 98 program suite [15]. The calculations were done at MP2(Full) level with a reasonably larger basis set, 6-311++G**. Initial geometries were chosen with H_2S positioned along both b and c axes of C_2H_4 and also with H or S pointing towards the center of C_2H_4. Frequency calculations were carried out to ensure that the optimized structure was a true minimum.

3. Results and discussion

3.1. Search and assignment

The rotational constants for $C_2H_4–H_2S$ were predicted both by comparing the rotational constants for several B$\cdots$HCl and B$\cdots$H$_2$S (where B = Ar, C_6H_6 and C_2H_4) complexes and by ab initio calculations. A comparison of several HF/HCl and H_2O/H_2S complexes indicates that the intermolecular distances are similar. As the masses are close as well, the rotational constants are quite similar for complexes containing these two molecules. For example, the B rotational constant for $C_6H_6–HCl$ and $C_6H_6–H_2S$ are 1237.7 MHz [16] and 1168.5 MHz [17], respectively, and that of Ar–HCl and Ar–H_2S are 1678.5 MHz [18] and 1681.4 MHz [19], respectively. Considering these similarities, it was expected that the $C_2H_4–H_2S$ rotational constants would be close to those of $C_2H_4–HCl$ [20] but certainly on the lower side. A search for $1_{01} \rightarrow 2_{02}$ transition was started at 8950 MHz as the same transition for $C_2H_4–HCl$ occurs at 8951.366 MHz. It turned out to be a long search with the transition finally observed at 7677.8 MHz, very close to that of $C_2H_4–Ar$ (7655.7 MHz) [21].

Each transition is split into four lines with a smaller splitting of <1 MHz and a larger splitting of several MHz. These transitions could be fit independently to a Watson Hamiltonian with only five constants (A, B, C, D_J and D_{JK}). The rotational transitions observed and the fitted constants for the four progressions are given in Tables 1 and 2, respectively. The rms deviation is an order of magnitude larger (30 kHz) than the experimental uncertainty. However, there is a clear trend in the residues with all the $K = 0$ lines having residues within experimental uncertainties and the two $K_p = 1$ lines showing equal and opposite residues. The $C_2H_4–H_2S$ is a nearly prolate asymmetric top with $\kappa = -0.9912$. A stick diagram of the $1_{01} \rightarrow 2_{02}$ transitions is shown in Fig. 1 for $C_2H_4–H_2S$ along with those of $C_2H_4–H_2O$ [22,23] and $C_2H_4–Ar$ [21]. The similarity between $C_2H_4–H_2S$ spectrum and a superposition of $C_2H_4–H_2O$ and $C_2H_4–Ar$ is evident. The $C_2H_4–D_2S$ and $C_2H_4–H_2^{34}S$ isotopomers exhibited similar four line pattern. The $C_2H_4–HDS$ showed only two lines with smaller splitting that is identical to $C_2H_4–D_2S$. The rotational constants for the progression corresponding to L2 in Table 1 for all four isotopomers are given in Table 3. The observed splittings are given in Table 4. The larger splitting can be readily assigned to some internal motion of H_2S, as it is missing for the HDS

Table 1
List of transitions observed for $C_2H_4–H_2S$ complex

Transitions	L1		L2		U1		U2	
	Observed freq. (MHz)	Res. (kHz)	Observed freq. (MHz)	Res. (kHz)	Observed freq. (MHz)	Res. (kHz)	Observed freq. (MHz)	Res. (kHz)
$0_{00}–1_{01}$	3839.2887	3.6	3839.5289	−1.4	3842.5789	2.4	3842.8441	0.8
$1_{11}–2_{12}$	7567.9895	−49.3	7568.2071	−56.1	7573.8046	−47.7	7574.0447	−49.6
$1_{01}–2_{02}$	7677.8746	−1.2	7678.3620	−1.6	7684.4786	0.3	7685.0082	−3.8
$1_{10}–2_{11}$	7779.9832	51.2	7780.7434	57.3	7788.0750	47.9	7788.9219	48.8
$2_{12}–3_{13}$	11350.9490	−31.9	11351.2883	−29.3	11359.7351	−28.6	11360.0947	−28.5
$2_{02}–3_{03}$	11515.0758	−1.7	11515.8051	2.4	11525.0275	−2.5	11525.8346	3.3
$2_{11}–3_{12}$	11668.8501	30.2	11669.9797	28.4	11681.0539	28.8	11682.3206	29.9
$3_{13}–4_{14}$	15132.6796	48.6	15133.1301	50.0	15144.5033	45.3	15144.9772	46.2
$3_{03}–4_{04}$	15350.1954	0.9	15351.1487	−0.6	15363.5568	1.1	15364.6246	−0.8
$3_{12}–4_{13}$	15556.3646	−48.3	15557.8716	−49.9	15572.7576	−45.5	15574.4373	−46.8

Table 2
Rotational and centrifugal distortion constants for C_2H_4–H_2S complex

Parameters	L1	L2	U1	U2
A (GHz)	26(1)	26(1)	26(1)	26(1)
B (MHz)	1972.64(1)	1972.90(1)	1974.86(1)	1975.14(1)
C (MHz)	1866.70(1)	1866.69(1)	1867.77(1)	1867.75(1)
D_J (kHz)	14.3(5)	14.3(5)	13.2(5)	13.3(5)
D_{JK} (MHz)	1.060(15)	1.061(16)	0.974(14)	0.971(14)
SD (kHz)	34.2	36.2	32.2	33.0
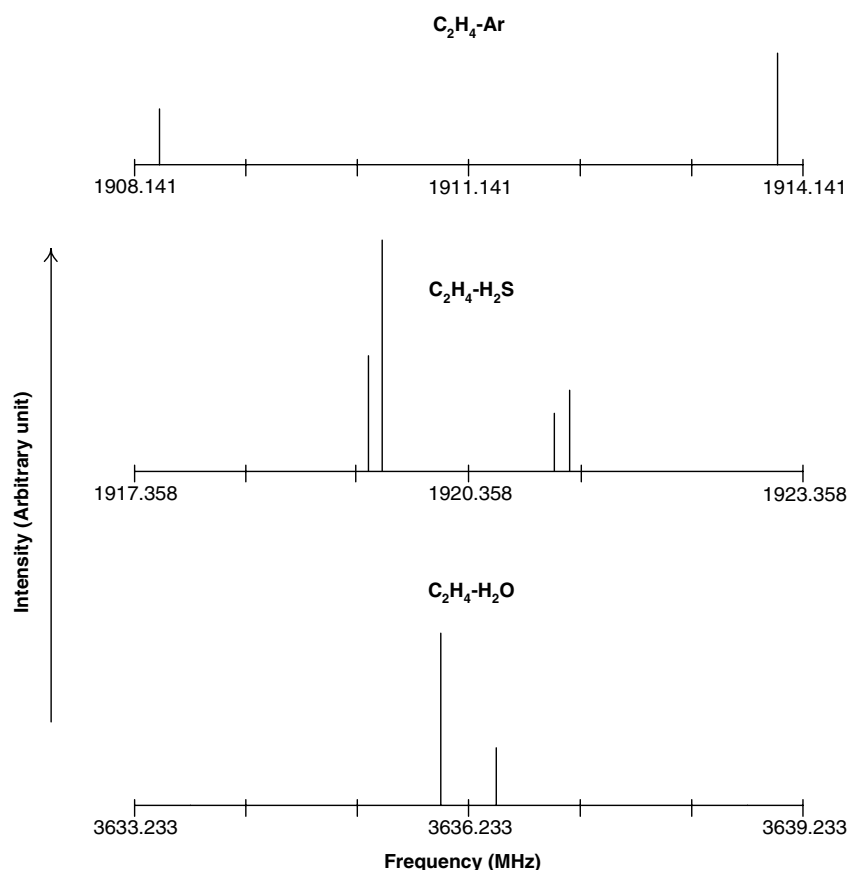
Fig. 1. Stick diagram of $J = 1 \rightarrow 2$, $K = 0$ transition frequencies for C_2H_4–Ar, C_2H_4–H_2S and C_2H_4–H_2O. The transition frequencies have been divided by $2(J + 1)$ (i.e. 4) in order to plot with the same scale.

Table 3
Rotational and centrifugal distortion constants for C_2H_4–H_2S isotopomers

Parameters	H_2S	HDS	D_2S	$H_2^{34}S$
A (GHz)	26(1)	26(1)	26(1)	26(1)
B (MHz)	1972.90(1)	1964.68(1)	1927.67(1)	1923.11(1)
C (MHz)	1866.69(1)	1859.50(1)	1830.30(1)	1822.05(1)
D_J (kHz)	14.3(5)	11.1(4)	11.8(5)	13.7(5)
D_{JK} (MHz)	1.061(16)	0.882(18)	0.925(13)	1.010(17)
SD (kHz)	34.2	47.8	46.9	33.0

complex. The splitting observed for D_2S is nearly twice that of H_2S, which rules out any tunneling mechanism. The C_6H_6–H_2O complex [24] exhibits similar splitting with the D_2O complex showing a splitting that is roughly twice that of H_2O. The smaller splitting observed is more intriguing. The fact that it is observed in HDS complex rules out tunneling/internal rotation of H_2S about any other axis. Internal rotation of the hy-

Table 4
Experimental splittings (in MHz) observed in $(B + C)/2$ for C_2H_4–H_2S isotopomers

Isotopomer	1–2	L–U
H_2S	0.14	1.67
$H_2^{34}S$	0.12	1.33
HDS	0.035	–
D_2S	0.035	3.11

drogen away from C_2H_4 about the S–H$\cdots\pi$ bond (see Fig. 2) is unlikely to be the cause, as both HDS and D_2S show identical splitting. Both HDS and D_2S are bonded through D atom and such rotation should involve H or D, respectively, and hence should lead to different splitting. Internal rotation of C_2H_4 about it's a-axis, as observed in C_2H_4–Ar complex [21] appears to be the most likely candidate. However, the splitting is dependent on isotopic substitutions on H_2S. It suggests that the internal rotation of C_2H_4 is accompanied by S–H bond contraction, which seems reasonable. Experimental data on substituted C_2H_4 and a detailed analysis of the potential energy surface for the different internal motions would be useful and we are currently working on both these aspects.

3.2. Structure from rotational constants and ab initio calculations

The A rotational constant is not well determined in the fit but within the uncertainty, it is identical for all
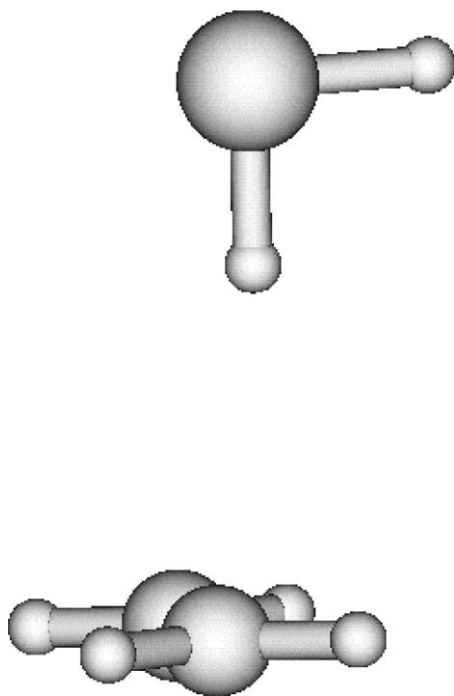

Fig. 2. The equilibrium geometry of C_2H_4–H_2S calculated at MP2/6-311++G** level.

four isotopomers and it is close to the C rotational constant for C_2H_4. It is similar for the structures determined for all C_2H_4–HX complexes (X = F [25], OH [22,23] and Cl [20]) and ab initio results presented here. The H_2S is located on the c-axis of C_2H_4 forming a 'hydrogen bond' with the π cloud. However, the B and C rotational constants are reasonably accurate and the c.m.–c.m. separation could be readily determined, assuming the monomer structures are unchanged in the complex. Using parallel axes theorem, one could write the following expressions for moments of inertia about b- and c-axes of the complex

$$I_b(\text{complex}) = I_a(C_2H_4) + I_a(H_2S) + \mu R^2 \qquad (1)$$

$$I_c(\text{complex}) = I_b(C_2H_4) + I_c(H_2S) + \mu R^2 \qquad (2)$$

Here, μ is the reduced mass of the complex and R is the c.m.–c.m. separation. The H_2S is assumed to be symmetrically bonded to C_2H_4. The R is calculated to be 4.041(1) and 4.037(1) Å, from Eqs. (1) and (2), respectively. Neglecting the contribution of H_2S (assuming it to be spherical) increases the R by 0.01 Å. As the H_2S term contributes the least to the moments of the complex, consideration of other orientations is unlikely to change the R significantly.

Substitution analysis based on the rotational constants for the various H_2S isotopomers can be used to locate the substituted atom more accurately [26]. From the rotational constants of C_2H_4–H_2S, C_2H_4–DHS, C_2H_4–D_2S and C_2H_4–$H_2^{34}S$, the c.m. to atom distances for H (bonded to C_2H_4), S and H (away from C_2H_4) were determined to be 1.034, 1.852 and 2.163 Å, respectively. Though, the D substitution results are less reliable compared to result from ^{34}S substitution, one unambiguous conclusion is that the H_2S is interacting through H with the π cloud. The equilibrium structure calculated at MP2(Full)/6-311++G** level theory is in agreement with this conclusion as shown in Fig. 2. Different initial guesses for the geometry, mentioned earlier, led to this same minimum. The rotational constants from the calculation are $A = 22945$ MHz, $B = 2008$ MHz and $c = 1917$ MHz compared to the experimental values of 26(1), 1972.64(1) and 1866.70(1) MHz, respectively.

Frequency calculations with the structure shown in Fig. 2 revealed that it is a true minimum. Also, a red shift in S–H stretching frequencies was observed. For comparison, S–H stretching frequencies calculated at MP2/6-311++G** level are listed in Table 5 for free H_2S, Ar–H_2S, H_2S–H_2S and C_2H_4–H_2S. The red-shifts observed in symmetric and asymmetric stretching frequencies are only 1–2 cm^{-1} for Ar–H_2S and for C_2H_4–H_2S, they are 11 and 9 cm^{-1}, respectively. Does the small shift observed for Ar–H_2S make it a hydrogen bonded complex? The frequency shifts calculated for $(H_2S)_2$ provide an answer. For H_2S–H_2S, the shifts

Table 5
Comparison of S–H stretching frequencies (in cm^{-1}) of free H$_2$S, Ar–H$_2$S, H$_2$S–H$_2$S[a] and C$_2$H$_4$–H$_2$S calculated at MP2(Full) level using 6-311++G**basis set

	S–H symmetric stretching	S–H asymmetric stretching
H$_2$S	2818	2838
Ar–H$_2$S	2817	2836
H$_2$S–H$_2$S(a)	2817	2836
H$_2$S–H$_2$S(d)	2806	2830
C$_2$H$_4$–H$_2$S	2807	2829

[a] Row 3 has values for acceptor H$_2$S and row 4 has values for donor H$_2$S.

Table 6
Binding energy (in kcal/mol) for C$_2$H$_4$–H$_2$S and Ar–H$_2$S complexes calculated at MP2(Full) level using 6-311++G** basis set

	C$_2$H$_4$–H$_2$S		Ar–H$_2$S	
	With BSSE	Without BSSE	With BSSE	Without BSSE
ΔE	−0.8763	−2.1316	0.0679	−0.4198
ΔE_{ZPE}	0.3196	−0.9362	0.2720	−0.2157

ΔE and ΔE_{ZPE} correspond to the zero-point energy uncorrected and zero-point energy corrected binding energies, respectively.

observed for acceptor H$_2$S are identical to those of Ar–H$_2$S and the shifts observed for donor H$_2$S are identical to those of C$_2$H$_4$–H$_2$S. The frequency shifts observed in C$_2$H$_4$–H$_2$S are quite comparable to the experimental shift of 16 cm^{-1} observed in dilute thiophenol solution in benzene [27]. These observations strongly support S–H$\cdots\pi$ interaction in C$_2$H$_4$–H$_2$S complex. The binding energies calculated for these two complexes are shown in Table 6. Binding energies were corrected for basis set superposition error (BSSE) using the counterpoise method [28] and for zero point energy (ZPE). Not surprisingly, zero point corrections reduce the binding energy for C$_2$H$_4$–H$_2$S and Ar–H$_2$S. The reduction is more for the former as there are six new vibrations in the complex compared to three for Ar–H$_2$S. For both complexes, the other vibrational frequencies are very close to those of the monomers. Without BSSE, the ZPE corrected binding energies are −0.22 and −0.94 kcal mol^{-1} for Ar–H$_2$S and C$_2$H$_4$–H$_2$S, respectively. The BSSE corrected values come out to be positive for both complexes at this level. Obviously, the counterpoise method for BSSE overcorrects, leading to artificial positive values for binding energy in these two cases.

4. Conclusions

Rotational spectrum of C$_2$H$_4$–H$_2$S is reported in this Communication. Each transition is split in to 4 components indicating that both C$_2$H$_4$ and H$_2$S exhibit large amplitude tunneling/internal rotation in the complex.

The splitting pattern observed for HDS and D$_2$S suggests that the larger splitting is due to internal rotation of H$_2$S and the smaller splitting is due to internal rotation/tunneling of C$_2$H$_4$ coupled to S–H stretching motion. The geometry and theoretical vibrational frequency shifts indicate C$_2$H$_4$–H$_2$S complex to be 'hydrogen bonded' like the other C$_2$H$_4$–HX (X = F, Cl, OH) complexes. However, the binding energy is small and the intermolecular potential is floppier for C$_2$H$_4$–H$_2$S than the other C$_2$H$_4$–HX complexes. Hence, ethylene tunneling has been experimentally observed in this complex similar to that observed for C$_2$H$_4$–Ar and unlike for the other C$_2$H$_4$–HX hydrogen bonded complexes mentioned above.

References

[1] C. Leforestier, F. Gatti, R.S. Fellers, R.J. Saykally, J. Chem. Phys. 117 (2002) 8710.
[2] R.C. Cohen, R.J. Saykally, Ann. Rev. Phys. Chem. 42 (1991) 369.
[3] T.H. Dunning Jr., J. Phys. Chem. A 104 (2000) 9062.
[4] R.F.W. Bader, Atoms in Molecules. A Quantum Theory, Clarendon Press, Oxford, 1990, p. 302.
[5] A.D. McNaught, A. Wilkinson, IUPAC Compendium of Chemical Terminology, second edn., Blackwell Science, Ltd., Oxford, 1997.
[6] F-M. Tao, W. Klemperer, J. Chem. Phys. 103 (1995) 950.
[7] J.D. Augspurger, C.E. Dykstra, Chem. Phys. Lett. 189 (1992) 303.
[8] P.K. Mandal, E. Arunan, J. Chem. Phys. 114 (2001) 3880.
[9] E. Arunan, A.P. Tiwari, P.K. Mandal, P.C. Mathias, Curr. Sci. 82 (2002) 533.
[10] C.H. Görbitz, B. Dalhus, Acta Crystallogr. C 52 (1996) 1756.
[11] T.J. Balle, W.H. Flygare, Rev. Sci. Instrum. 52 (1981) 33.
[12] J.-U. Grabow, W. Stahl, H. Dreizler, Rev. Sci. Instrum. 67 (1996) 4072.
[13] R.D. Suenram, J.-U. Grabow, A. Zuban, I.A. Leonov, Rev. Sci. Instrum. 70 (1999) 2127.
[14] E. Arunan, Sagarika Dev, P.K. Mandal, App. Spectrosc. Rev. 39 (2004) 131.
[15] M.J. Frisch et al., GAUSSIAN 98, Revision A.11.3, Gaussian, Inc., Pittsburgh, PA, 2002.
[16] W.G. Read, E.J. Campbell, G. Henderson, J. Chem. Phys. 78 (1983) 3501.
[17] E. Arunan, T. Emilsson, H.S. Gutowsky, G.T. Fraser, G. de Oliveira, C.E. Dykstra, J. Chem. Phys. 117 (2002) 9766.
[18] S.E. Novick, P. Davies, S.J. Harris, W. Klemperer, J. Chem. Phys. 59 (1973) 2273.
[19] H.S. Gutowsky, T. Emilsson, E. Arunan, J. Chem. Phys. 106 (1997) 5309.
[20] P.D. Aldrich, A.C. Legon, W.H. Flygare, J. Chem. Phys. 75 (1981) 2126.

[21] Y. Liu, W. Jäger, J. Chem. Phys. 119 (2003) 8449.

[22] K.I. Peterson, W. Klemperor, J. Chem. Phys. 85 (1986) 725.

[23] A.M. Andrews, R.L. Kuczkowski, J. Chem. Phys. 98 (1993) 791.

[24] H.S. Gutowsky, T. Emilsson, E. Arunan, J. Chem. Phys. 99 (1993) 4883.

[25] J.A. Shea, W.H. Flygare, J. Chem. Phys. 76 (1982) 4857.

[26] W. Gordy, R.L. Cook, Microwave Molecular Spectra, third edn., Wiley, New York, 1984, p. 663.

[27] J.G. David, H.E. Hallam, Spectrochimica Acta 21 (1965) 841, as quoted in G.R. Desiraju, T. Steiner, The Weak Hydrogen Bond, Oxford University Press, 1999 p. 254.

[28] S.F. Boys, F. Bernardi, Mol. Phys. 19 (1970) 553.